

9.2 Neutral Points of Skylight Polarization Observed During the Totality of the Eclipse on 11 August 1999

In spite of the scientific popularity of total solar eclipses, appearing almost every year somewhere on the earth, the empirical knowledge accumulated about the polarization pattern and neutral points of eclipse skies is rather limited, since the earlier polarization measurements were restricted to one single point in the sky or at most to the solar and antisolar meridian. Due to the methods of full-sky imaging polarimetry (North and Duggin 1997; Voss and Liu 1997; Liu and Voss 1997; Gál et al. 2001a,b,c; Pomozi et al. 2001a,b; Horváth et al. 2002a,b) the last difficulty was cleared away to measure the polarization pattern of the entire skydome under the extreme illumination conditions occurring during the short period of a total solar eclipse. Horváth et al. (2003) reported on the neutral points of the eclipse sky observed on 11 August 1999 in Hungary.

In this chapter observational material is presented about the neutral points and local minima of the degree of linear polarization p of the eclipse sky collected by Horváth et al. (2003). Earlier only de Bary et al. (1961) observed exactly zero p of skylight during totality at 90° from the obscured sun on the antisolar meridian. Numerical calculations of the atmospheric scattering phenomena under the complex illumination conditions of the eclipse on 11 August 1999 with the use of an improved version of the quantitative model of Können (1987) could be an interesting task of future work. We refer to the sky observed immediately before or after totality (immediately before the second contact or after the third contact) of the solar eclipse as "preeclipse sky" or "posteclipse sky", respectively. Under "normal sky" we mean the sky observed under normal illumination conditions when the sun was not eclipsed by the moon, but its zenith angle was the same (32°) as that during totality on 11 August 1999.

Figures 9.2.1 and 9.2.2 show the celestial patterns of p and α of skylight measured at two different moments (see Fig. 9.1.1B) at 450 and 550 nm during totality. Figures 9.2.3 and 9.2.4 represent the graphs of p and α measured along different meridians crossing the zenith and the neutral points or the local minima of p listed in Table 9.2.1. One of the most striking features of the α -pattern of the eclipse sky (Fig. 9.2.2) is that α changes from 0° (or from 180° because of the 180° periodicity of α) to 90° near the zenith if the direction of view moves approximately along the solar and antisolar meridian. Other remarkable phenomenon in the eclipse sky is the occurrence of points, where p is zero or has a local minimum (Figs. 9.2.1 and 9.2.3). Table 9.2.1 summarizes the zenith angles θ and azimuth angles φ (measured counter-clockwise from West) of these celestial points.

On the p -patterns measured at 12:51:34 (Figs. 9.2.1A, 9.2.3B) and 12:52:00 (Figs. 9.2.1B, 9.2.3D) at 450 nm a point is discernible near the zenith where $p = 0\%$. This point is called "zenith neutral point of type-2". It is called neutral point,

because p is zero at it; and it is classified as "type-2", because it can be considered a point where p passes through a minimum, rather than a real neutral point as the well-known Arago, Babinet and Brewster neutral points of the normal sky classified as "type-1" further on. In the type-2 zenith neutral point of the eclipse sky the absence of polarization is analogous to the absence of polarization of the sunlit sky straight in the direction of the sun. At 12:52:00 approximately at the position of the zenith neutral point a local minimum of p occurred at 550 nm (Figs. 9.2.1C, 9.2.3F). The local minimum of p in the immediate vicinity of the zenith can also be seen in the graphs of Figs. 9.2.3A, 9.2.3C and 9.2.3E.

At 12:51:34 at 450 nm (Figs. 9.2.1A and 9.2.3A) two neutral points of type-1 occurred approximately along the antisolar meridian near the horizon. They arise because the Stokes parameter Q (if $U = 0$) for single and multiple (double) scattering cancels out, that occurs also in the usual Arago, Babinet and Brewster neutral points (Coulson 1988; Gál et al. 2001a,c; Horváth et al. 1998b; Horváth and Wehner 1999).

At 12:52:00 a neutral point of type-3 was observed at 450 nm (Figs. 9.2.1B, 9.2.3C) and a local minimum of p occurred at 550 nm (Figs. 9.2.1C, 9.2.3E) approximately at the position of the two type-1 neutral points. Note that there was no switch of α crossing the type-3 neutral point along a meridian: this celestial point is characterized by the abolition of p (Figs. 9.2.1B, 9.2.3C) in a celestial area where the α -pattern is homogeneous, that is, the E-vectors are approximately horizontal on both sides of the neutral point (Figs. 9.2.2B, 9.2.4C). The latter feature distinguishes the neutral point of type-3 from the neutral points of type-1 and type-2, which are characterized by a sudden change of 90° of α (Figs. 9.2.2A, 9.2.2B, 9.2.4A, 9.2.4B, 9.2.4D).

9.2.1 Origin of the Zenith Neutral Point During Totality

Figure 9.2.5 explains qualitatively the origin of the neutral point or local minimum of p observed near the zenith during totality of the eclipse on 11 August 1999. This qualitative model is similar to that discussed in Chapter 9.1. If only primary (B_1) and second order (B_2) scattering events are taken into account, the situation is shown in Fig. 9.2.5A. Since the atmospheric scattering centres (B_2) at or near the zenith (above the observer in the umbra) are illuminated by single-scattered Rayleigh skylight with all possible directions of the E-vector coming from outside the umbra (B_1), the atmosphere at or near the zenith scatters E-vectors with all possible alignments towards the observer. This results in a zero or almost zero net p , that is, unpolarized skylight or skylight with very low p near the zenith. If beside first (B_1) and second (B_2) order scattering also third order scattering events (B_3) are taken into account, the situation is shown in Fig. 9.2.5B. In the umbra, from the northern (Fig. 9.2.5B4) or southern (Fig. 9.2.5B2) part of the sky (B_2) the atmospheric scattering centres (B_3) above the observer (at or near the zenith) are illuminated mainly by highly polarized scattered Rayleigh skylight (B_1), the E-vectors of which are approximately perpendicular or parallel to the local meridian, respectively. From the western (Fig. 9.2.5B1) or eastern (Fig. 9.2.5B3) part of the

sky (B_2) the atmospheric scattering centres at or near the zenith (B_3) are illuminated mainly by more or less polarized scattered Rayleigh skylight (B_1), the E-vectors of which are more or less diagonal relative to the local meridian. These more or less perpendicularly, parallelly and diagonally polarized rays of skylight are scattered from the zenith (B_3) towards the observer (Fig. 9.2.5B5) resulting in all possible directions of the E-vector. This results in again unpolarized skylight or skylight with very low p at or near the zenith.

The exact position of the zenith neutral point or local minimum of p near the zenith depends on the wavelength (due to the dispersion of polarization of scattered skylight) as well as on the time-dependent geometry of the lunar shadow with respect to the earth's surface and the observer's position. Shaw (1975) observed a similar minimum of p in the eclipse sky, which phenomenon was quantitatively explained by Können (1987).

9.2.2 Origin of Another Neutral Points at Totality

The prerequisite of formation of a neutral point or a local reduction of p in the positively polarized antisolar half of the sky during totality is a mechanism that introduces negatively polarized light into the umbral region of the atmosphere. One of such mechanisms is the reflection of light from the ground. Natural soil surfaces reflect more or less partially linearly polarized light, the p of which depends on the type (roughness, albedo and spectral characteristics) of the surface (Coulson 1974). It is a general rule that the higher the albedo of a rough reflecting surface in a given spectral range, the lower the p of reflected light. This phenomenon is called the Umov effect (Coulson 1988). The polarization of the ground-reflected light is negative or positive if the angle of reflection measured from the direction of incidence is smaller or greater than a threshold angle γ , respectively (Fig. 9.1.6A). Angle γ is dependent on the characteristics of the reflecting surface, but its typical value is about 20° for bright sandy and grassy terrains, as was the terrain at the place of the polarimetric measurements of Horváth et al. (2003) in the surroundings of Kecel (Hungary). The degree of negative polarization of light reflected from such a surface changes from zero to several percents if the angle of reflection with respect to the direction of incidence decreases from γ to zero.

Figure 9.1.6A shows schematically the situation when such negatively or positively polarized ground-reflected light is introduced into the atmosphere during the total eclipse. The degree of positive polarization of multiply scattered skylight from the antisolar half of the sky in the umbra is more or less reduced by the negatively and enhanced by the positively polarized light reflected by the ground from outside the umbral region if it is scattered towards the observer by umbral atmospheric scattering centres (n_- and n_+ in Fig. 9.1.6A). At a given direction of view depending on the relative intensity of the positively and negatively polarized skylight (the Stokes parameter Q if $U = 0$), the following three different situations can be imagined:

1. If at wavelength λ the negatively polarized skylight intensity $I_-(\lambda)$ is smaller than the positively polarized skylight intensity $I_+(\lambda)$ in all directions of view, a local minimum of the celestial degree of positive polarization can be observed at the zenith angle of the maximum reduction of p (Figs. 9.2.1C, 9.2.3E).
2. If $I_-(\lambda) = I_+(\lambda)$ at a certain zenith distance, a neutral point occurs in this direction (Figs. 9.2.1B, 9.2.3C).
3. If $I_-(\lambda) > I_+(\lambda)$, a negatively polarized "island" is seen in the region of positive polarization (Figs. 9.2.1A, 9.2.2A, 9.2.3A, 9.2.4A). Then two neutral points appear at the border of this celestial island of negative polarization. In these neutral points the positive polarization switches to negative polarization as in the case of the neutral point observed near the zenith during totality, or of the normal Arago, Babinet and Brewster neutral points.

Due to the moving lunar shadow both the p - and α -patterns change during totality for any location of the observer while the eclipse proceeds from 2nd to 3rd contact. These changes depend on the wavelength and are determined by the observer's view through a varying slant range of air in the umbra, before the directly scattered sunlight is encountered. The site and points of time of the measurements of Horváth et al. (2003) in relation to the moving umbra as well as the wavelengths (450, 550 nm) of their observations were so fortunate during the totality of the eclipse on 11 August 1999 that they could observe all the above-mentioned three different situations (Figs. 9.2.1-9.2.4). In these cases the maximum reduction of p happened approximately along the antisolar meridian, because the thickness of the umbral region of the atmosphere receiving negatively polarized ground-reflected light was the greatest in this direction at the time of recording.

It is interesting that in the special case when condition 1 was satisfied there was no switch of α crossing the neutral point of type-3 along a meridian. This unique celestial point is characterized by the abolition of p in a celestial area where the α -pattern is homogeneous, that is, positive polarization occurs on both sides of the neutral point. The latter feature distinguishes this unique neutral point of type-3 from the other neutral points of type-1 and type-2 of the eclipse sky as well as from the normal Arago, Babinet, Brewster and fourth neutral points, which are characterized by a sudden change of 90° of α .

During the total eclipse on 11 August 1999 in Kecel the degree of negative polarization of multiply scattered skylight from the solar half of the sky in the umbra was more or less enhanced by the negatively and reduced by the positively polarized light reflected by the ground from outside the umbral region and scattered towards the observer by umbral atmospheric scattering centres (m_- and m_+ in Fig. 9.1.6A). During totality the negatively polarized light dominated in the solar half of the firmament, thus here negatively polarized skylight with slightly greater p than in the antisolar half was observed.

The main cause of the slight drift of the neutral points from the solar-antisolar meridian (Table 9.2.1) may be the changing geometry of the umbra with respect to the observer as the eclipse proceeded. A second cause may be distant clouds,

which may disturb the distribution of singly scattered light around the observer. A third factor is the polarization of singly scattered light. Such effects may be capable to explain the observed double neutral points, but calculations should prove this conjecture in the future.

9.2.3 Relation of the Unique Neutral Point Observed During the Eclipse on 11 August 1999 to Earlier Observations on Anomalous Neutral Points

The oldest report on an anomalous neutral point dates back to Brewster (1864), who on 22 occasions observed a dark purple band extending to 1.5° above the sea horizon at the azimuth of the antisun. This band had positive polarization, instead of the usual negative polarization existing between the Arago point and horizon. Due to this positively polarized horizontal band a secondary Arago point occurred at the edge of the band. Generally, the normal Arago point and the band of positive polarization near the horizon were separated by a band of negative polarization with the primary and secondary Arago points well defined. This phenomenon was most often seen above a sea horizon, it occasionally occurred above a land horizon as well. In one special case when the primary Arago point coincided with the edge of the band, a strange situation occurred in which the Arago point had positive polarization on both sides of it.

The latter observation of Brewster (1864) recalls the celestial distribution of polarization around the unique neutral point of type-3 observed by Horváth et al. (2003) on 11 August 1999 in the eclipsed sky: also this unique neutral point occurred in a positively polarized celestial region near the (land) horizon, approximately along the antisolar meridian. Both neutral points observed by Brewster and Horváth et al. (2003) differ from the normal Arago, Babinet and Brewster points, because the latter occur always at the edge of positively and negatively polarized neighbouring regions rather than in a positively polarized area of the sky.

The change of sky polarization that occurs during totality is complex and depends on the distribution and magnitude of numerous parameters: e.g. variations in ground albedo, solar zenith angle, shape and diameter of the eclipse shadow (umbra) and optical thickness of the atmosphere. Due to the complex geometry and the great number of control parameters, apart from the quantitative model of skylight polarization developed by Können (1987) for solar eclipses, at present does not exist any in-depth computation for determining the celestial polarization during an eclipse. According to Können (1987, p. 607): "Within the limited set of existing observations there is no possibility to test the model further at present. This has to wait until more detailed observations are available. Such observations should include the polarization distribution of the eclipse sky, preferably in the solar vertical plane and in the plane perpendicular to the solar vertical containing the zenith, together with simultaneous almucantar scans of radiance and polarization near the horizon, all of them preferably at various wavelengths. Only if such a complete set of measurements is available will a rigorous test of models

like the present one be possible." Full-sky imaging polarimetry meets these requirements, and the polarimetric data gathered by Pomozi et al. (2001a) and Horváth et al. (2003) make possible to test any quantitative model of the polarization of eclipsed skies.

The ground-based observation of total solar eclipses is regarded by many scientists as the fuss of amateurs and its scientific importance is frequently queried too. The results obtained by full-sky imaging polarimetry (Pomozi et al. 2001a; Horváth et al. 2003) demonstrate, however, that the ground-based study of eclipses can even nowadays yield new scientific issues.

Table

Table 9.2.1. Zenith angles θ and azimuth angles φ (measured counter-clockwise from West; for the antisolar meridian: $\varphi_{a.m.} = 79^\circ$) of the local minima of the degree of linear polarization p and the neutral points of skylight polarization observed during the total solar eclipse on 11 August 1999 in Kecel (Hungary). The numerical values are given in format $a \pm b$, where a is the average and b is its standard deviation. (After Table 2 of Horváth et al. 2003, p. 474).

circular patterns in Figs. graphs in Figs.	9.2.1A, 9.2.2A 9.2.3A, 9.2.3B, 9.2.4A, 9.2.4B	9.2.1B, 9.2.2B 9.2.3C, 9.2.3D, 9.2.4C, 9.2.4D	9.2.1C, 9.2.2C 9.2.3E, 9.2.3F, 9.2.4E, 9.2.4F
recording time	12:51:34	12:52:00	12:52:00
wavelength	450 nm (blue)	450 nm (blue)	550 nm (green)
neutral point N2 of type-2 near the zenith	$\theta = 14^\circ \pm 2^\circ$ $\varphi = 76^\circ \pm 3^\circ$	$\theta = 5^\circ \pm 2^\circ$ $\varphi = 74^\circ \pm 3^\circ$	– –
first neutral point N1 of type-1 near the horizon	$\theta = 60^\circ \pm 2^\circ$ $\varphi = 74^\circ \pm 3^\circ$	– –	– –
second neutral point N1 of type-1 near the horizon	$\theta = 66^\circ \pm 2^\circ$ $\varphi = 74^\circ \pm 3^\circ$	– –	– –
neutral point N3 of type-3 near the horizon	– –	$\theta = 64^\circ \pm 2^\circ$ $\varphi = 85^\circ \pm 2^\circ$	– –
local minimum MH of p near the horizon	– –	– –	$\theta = 67^\circ \pm 2^\circ$ $\varphi = 83^\circ \pm 2^\circ$
local minimum MZ of p near the zenith	– –	– –	$\theta = 4^\circ \pm 2^\circ$ $\varphi = 75^\circ \pm 2^\circ$

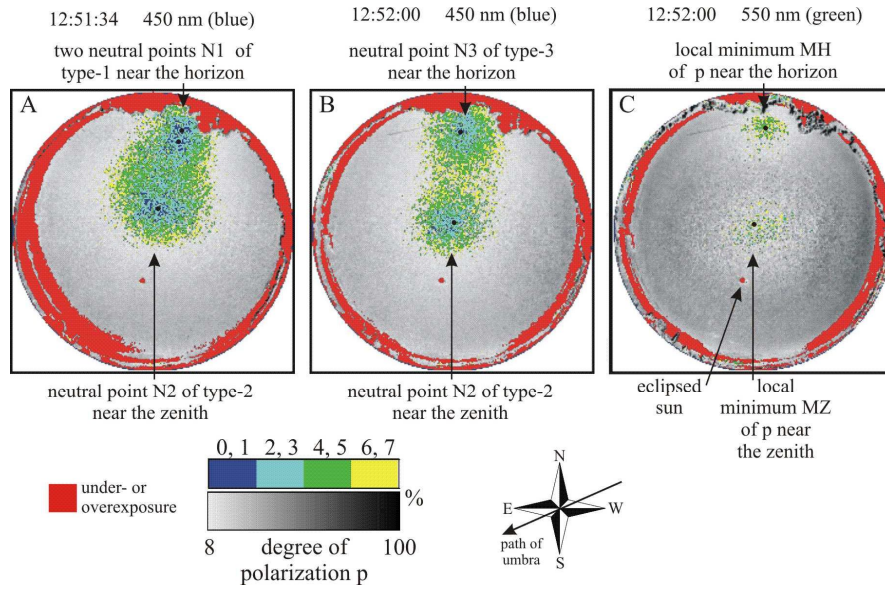


Fig. 9.2.1. Celestial patterns of the degree of linear polarization p of skylight measured with full-sky imaging polarimetry during totality of the solar eclipse on 11 August 1999 in Kecel (Hungary) at different times and wavelengths. A: 12:51:34 (local summer time = UTC+2), 450 nm; B: 12:52:00, 450 nm; C: 12:52:00, 550 nm. The values of p are rounded to integers (0,1,2,3,...,100%). The neutral points are marked by dots. (After Figs. 7-9 of Horváth et al. 2003, p. 469).

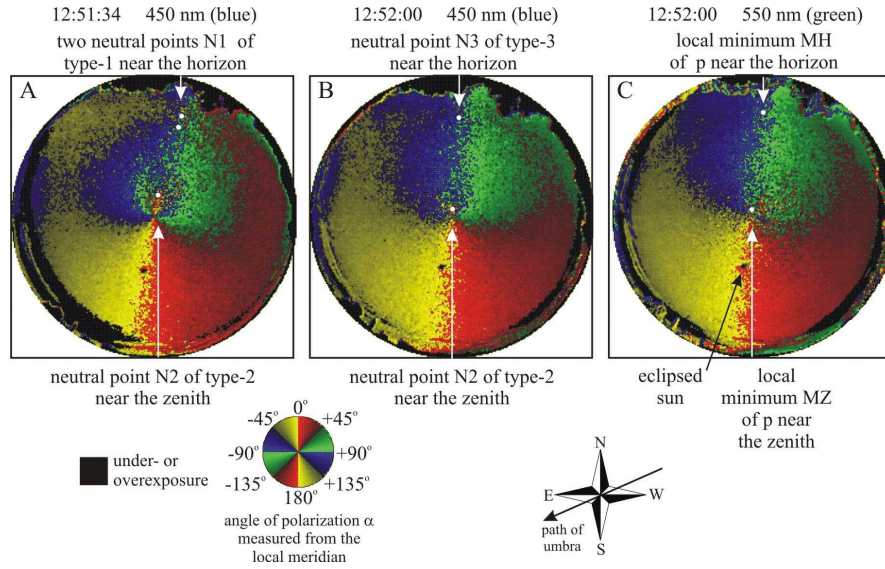


Fig. 9.2.2. As Fig. 9.2.1 for the angle of polarization α of skylight measured from the local meridian. (After Figs. 10-12 of Horváth et al. 2003, p. 469, 470).

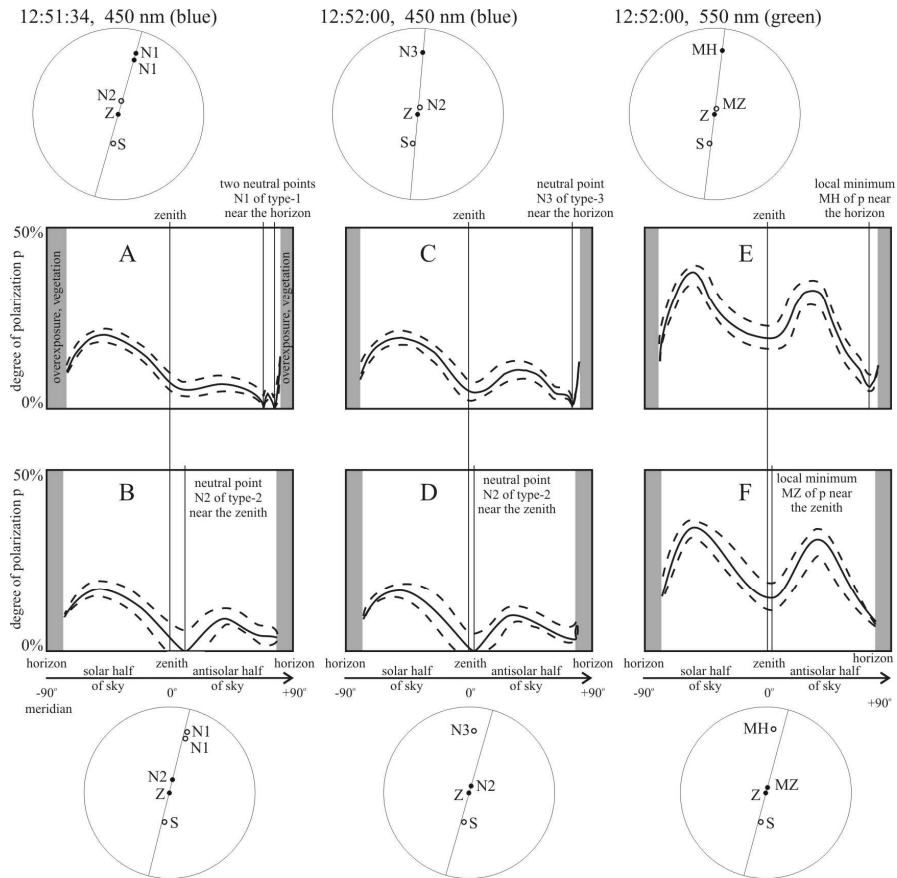


Fig. 9.2.3. Graphs of the degree of linear polarization p measured along different meridians crossing the zenith Z of the eclipse sky at different times and wavelengths. A, B: 12:51:34 (UTC+2), 450 nm; C, D: 12:52:00, 450 nm; E, F: 12:52:00, 550 nm. The continuous lines represent the curves fitted by the method of least squares to the measured values of p , while the dashed lines show the upper and lower limits, between which 90% of the p -values falls. The circular insets show how the scans are located relative to the circular patterns in Fig. 9.2.1. A: Scan through the two neutral points $N1$ of type-1 near the horizon. B: Scan through the neutral point $N2$ of type-2 near the zenith. C: Scan through the neutral point $N3$ of type-3 near the horizon. D: Scan through the neutral point $N2$ of type-2 near the zenith. E: Scan through the local minimum MH of p near the horizon. F: Scan through the local minimum MZ of p near the zenith. (After Figs. 13-15 of Horváth et al. 2003, p. 470, 471).

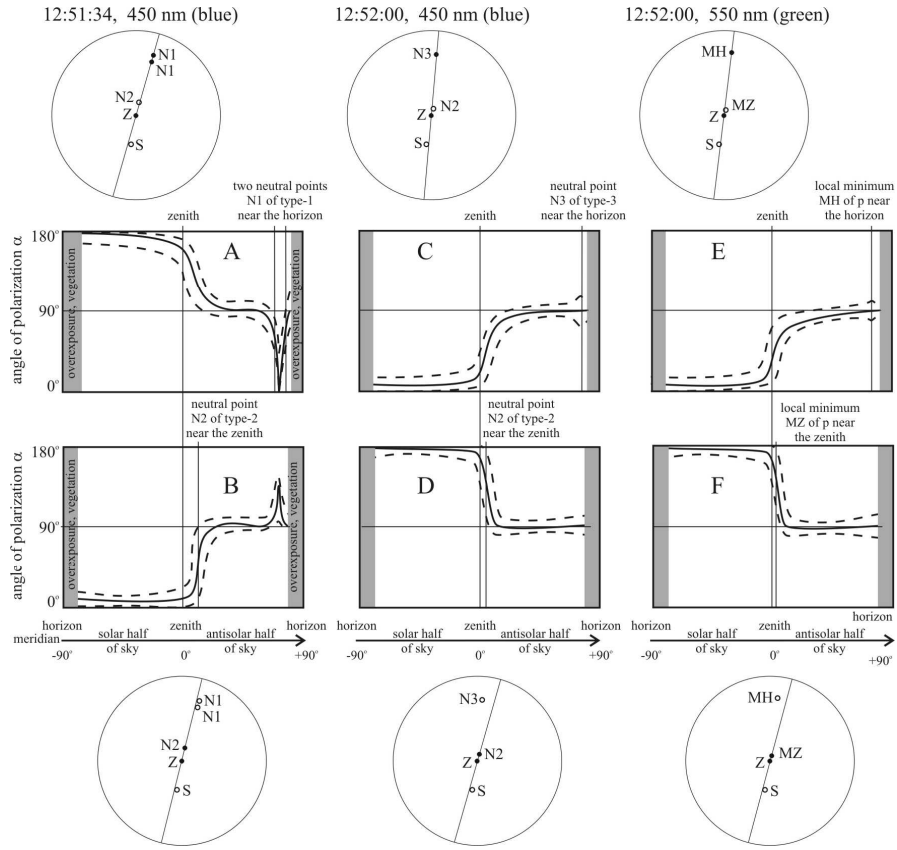


Fig. 9.2.4. As Fig. 9.2.3 for the angle of polarization α measured from the local meridian. (After Figs. 16-18 of Horváth et al. 2003, p. 472, 473).

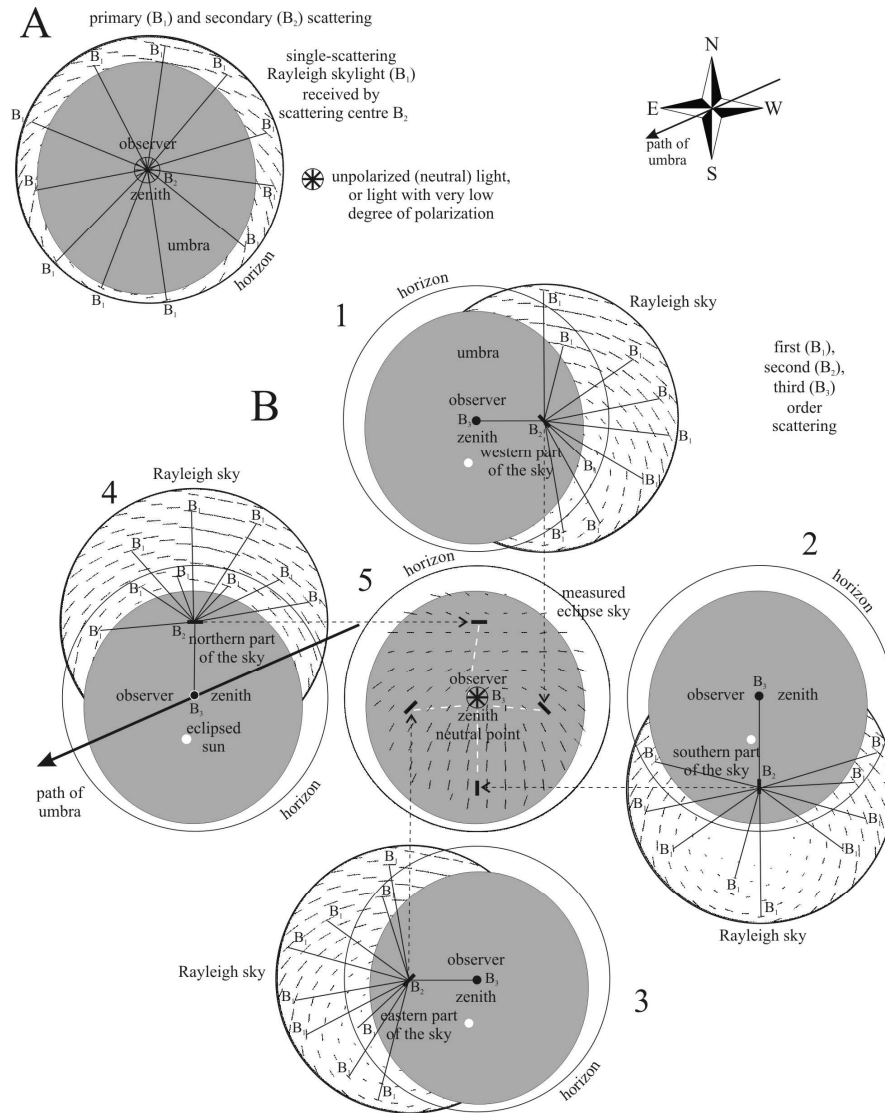


Fig. 9.2.5. For the qualitative explanation of the origin of the neutral point of skylight polarization observed near the zenith during totality if first and second order scattering events (A), or first, second and third order scattering events (B) are taken into account. (After Fig. 9 of Pomozi et al. 2001a, p. 198).